

## Neutron and X-Ray Diffraction Study on Polymorphism in Lithium Orthotantalate, $\text{Li}_3\text{TaO}_4$

M. ZOCCHI AND M. GATTI

*Dipartimento di Chimica Industriale ed Ingegneria Chimica del Politecnico,  
Piazza Leonardo da Vinci 32, 20133 Milan, Italy*

AND A. SANTORO AND R. S. ROTH

*National Measurement Laboratory, National Bureau of Standards,  
Washington, D.C. 20234*

Received December 2, 1982; in revised form March 17, 1983

The structures of the low- and high-temperature modifications of lithium orthotantalate,  $\text{Li}_3\text{TaO}_4$ , have been determined by neutron and X-ray diffraction methods. The low-temperature, or  $\beta$ , phase has symmetry  $C2/c$  and lattice parameters  $a_l = 8.500(3)$ ,  $b_l = 8.500(3)$ ,  $c_l = 9.344(3)$  Å, and  $\beta = 117.05(2)^\circ$ . The high-temperature, or  $\alpha$ , phase has symmetry  $P2$  and lattice parameters  $a_h = 6.018(1)$ ,  $b_h = 5.995(1)$ ,  $c_h = 12.865(2)$  Å, and  $\beta_h = 103.53(2)^\circ$ . Both structures are ordered. The  $\beta$ -phase has a rock salt-type structure with a 3:1 ordering of the  $\text{Li}^+$  and  $\text{Ta}^{5+}$  ions. Its structure can be generated from the low-temperature modification by means of a complex pattern of shifts of the  $\text{Ta}^{5+}$  ions.

### Introduction

The structure of lithium orthotantalate,  $\text{Li}_3\text{TaO}_4$ , has been investigated by Blasse (1) who found that the crystal is pseudotetragonal with a unit cell of parameters  $a_l = 6.01$  Å and  $c_l = 16.67$  Å. The  $\text{Ta}^{5+}$  ions were located by using X-ray powder diffraction intensities, and their arrangement suggested a 3:1 ordering of the  $\text{Li}^+$  and  $\text{Ta}^{5+}$  ions in a rock salt-type structure having a subcell of parameter  $a_c$  related to the parameters  $a_l$  and  $c_l$  by the expressions  $a_l = b_l = a_c\sqrt{2}$  and  $c_l = 4a_c$ .

A disordered rock salt phase of  $\text{Li}_3\text{TaO}_4$  of lattice parameter  $a_c = 4.203$  Å has been reported by Lapicky and Simanov (2) and by Pfeiffer (3). Blasse (1), however, was unable to prepare this modification by

quenching in water samples of the orthotantalate from 1000°C.

Martel and Roth (4) have found that  $\text{Li}_3\text{TaO}_4$  is, in fact, trimorphic, with the first-phase transition occurring at about 900°C and the second between 1400 and 1450°C. The low-temperature phase was found to have the same lattice parameters as the modification described by Blasse (1). The transition at about 900°C was detected in a differential thermal analysis pattern. This intermediate temperature phase could not be obtained at room temperature by quenching and, quite likely, is the same modification as that reported by Lapicky and Simanov (2) and by Pfeiffer (3). Martel and Roth (4) found that the high-temperature phase had symmetry lower than tetragonal.

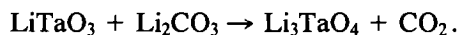
TABLE I  
EXPERIMENTAL CONDITIONS USED TO COLLECT THE NEUTRON POWDER INTENSITY DATA FOR  
THE  $\alpha$ - AND  $\beta$ -FORMS OF  $\text{Li}_3\text{TaO}_4$

Monochromatic beam	Reflection 220 of a Cu monochromator
Wavelength	1.5416(3) Å
Horizontal divergences	(a) In-pile collimator: 10' arc (b) Monochromatic beam collimator: 20' arc (c) Diffracted beam collimator: 10' arc ~15' arc
Monochromator mosaic spread	Vanadium can ~10 mm in diameter
Sample container	10–40, 30–60, 50–80, 70–100, 90–120
Angular ranges scanned by each detector	0.05°
Angular step	

Our purpose in beginning this work was to verify, complete, and refine Blasse's model for the low-temperature phase (referred to in what follows as the  $\beta$ -phase), and to solve the structure of the high-temperature form (called  $\alpha$ -phase in what follows). No attempts have been made to obtain and analyze the intermediate temperature modification. Both neutron powder and X-ray single-crystal diffraction methods have been used in the present study.

### Experimental

The orthotantalate was prepared by reacting lithium metatantalate and lithium carbonate according to the scheme:



The  $\beta$ -form was obtained by heating the mixture of  $\text{LiTaO}_3$  and  $\text{Li}_2\text{CO}_3$  at 700°C for 20 hr, at 800°C for 120 hr, and at 1000°C for 17 hr. The  $\alpha$ -form was prepared by heating the same starting materials at 800°C for 16 hr, at 1000°C for 23 hr, and at 1450°C for 2 hr. In both cases, after each thermal treatment, the resulting material was ground and analyzed by X-ray powder diffraction to monitor the progress of the reaction. The final products were pulled out of the furnace and cooled in air.

Neutron powder diffraction measure-

ments were made at room temperature with the high-resolution five-detector diffractometer at the National Bureau of Standards Reactor (5), using the experimental conditions indicated in Table I. The data were analyzed with the Rietveld method (6), modified by Prince (7) to simultaneously process the intensities collected by the five counters of the diffractometer. In the refinements based on the neutron data, the scattering amplitudes used were  $b(\text{O}) = 0.58$ ,  $b(\text{Li}) = -0.214$ , and  $b(\text{Ta}) = 0.70 \times 10^{-12}$  cm (8). The background was assumed to be a straight line of finite slope and was refined for each of the five channels of the diffractometer together with the profile and the structural parameters. A Gaussian peak shape was assumed in all cases since all the single reflections present in both powder patterns showed no broad tails.

X-ray intensity data on a single crystal of  $\alpha$ - $\text{Li}_3\text{TaO}_4$  were collected with a CAD-4 NONIUS four-circle diffractometer using  $\text{MoK}\alpha$  radiation ( $\lambda = 0.71069$  Å) and the  $\theta$ - $2\theta$  scan method. The crystal used in the experiment had a regular shape with an average diameter smaller than 0.1 mm. A total of 4025 reflections were measured. Of these, 3746 had intensities larger than  $3\sigma$  and were considered observed. Empirical absorption corrections and Lorentz-polarization factors were evaluated with standard NONIUS programs.

## Derivation and Refinement of the Models

### (a) $\beta$ -Phase

As required by the rock salt structure, the oxygen atoms are located at  $\frac{1}{2} 0 0$ ,  $0 \frac{1}{2} 0$ ,  $0 0 \frac{1}{2}$ , and  $\frac{1}{2} \frac{1}{2} \frac{1}{2}$ , using the fcc cell of parameter  $a_c$  as reference system. The location of the cations can be best specified in the pseudo-tetragonal cell introduced by Blasse (1) to describe the periodicity caused by the 3:1 ordering of the  $\text{Li}^+$  and  $\text{Ta}^{5+}$  ions. The transformation from the fcc lattice C to the pseudo-tetragonal lattice T is given by the matrix<sup>1</sup>

$$S_{ct} = (110/\bar{1}10/004).$$

In this new reference system, the  $\text{Ta}^{5+}$  ions are located at  $\frac{1}{4} \frac{1}{2} 0$ ,  $\frac{1}{2} \frac{1}{4} \frac{1}{2}$ ,  $\frac{3}{4} \frac{1}{2} \frac{1}{2}$ ,  $\frac{1}{2} \frac{3}{4} \frac{1}{2}$ ,  $\frac{3}{4} 0 \frac{1}{2}$ ,  $0 \frac{3}{4} \frac{1}{2}$ ,  $\frac{1}{4} 0 \frac{3}{4}$ , and  $0 \frac{1}{4} \frac{3}{4}$ , i.e., at the centers of one-fourth of the octahedra formed by the oxygen ions (see Fig. 2). The lithium ions could not be found by Blasse (1), and therefore, in a first trial model, they were located at the centers of the oxygen octahedra left empty after arranging the  $\text{Ta}^{5+}$  ions.

With this ordering of the atoms, the symmetry of the structure is  $C2/c$  with the two-fold axis parallel to the direction  $[1\bar{1}0]$  of the pseudo-tetragonal cell. The transformation matrix from the pseudo-tetragonal lattice T to the monoclinic lattice L is

$$S_{tl} = (\bar{1} \bar{1} 0/1 \bar{1} 0/\frac{1}{2} \frac{1}{2} \frac{1}{2}).$$

This trial model was refined with the Rietveld method, and the results are reported in Table II. Figure 1 shows the calculated and

<sup>1</sup> In our notation a matrix

$$S_{ab} = \begin{pmatrix} s_{11} & s_{12} & s_{13} \\ s_{21} & s_{22} & s_{23} \\ s_{31} & s_{32} & s_{33} \end{pmatrix}$$

performs the axes transformation

$$\begin{pmatrix} \tilde{a}_b \\ \tilde{b}_b \\ \tilde{c}_b \end{pmatrix} = S_{ab} \begin{pmatrix} \tilde{a}_a \\ \tilde{b}_a \\ \tilde{c}_a \end{pmatrix}.$$

TABLE II

RESULTS OF THE RIETVELD REFINEMENT OF THE STRUCTURE OF  $\beta\text{-Li}_3\text{TaO}_4$

Atom	x	y	z	B ( $\text{\AA}^2$ )
Ta	0.075(2)	-0.126(1)	0.123(2)	1.07(7)
Li(1)	0.329(4)	-0.116(5)	0.607(3)	0.8(2)
Li(2)	0.567(6)	-0.132(4)	0.107(4)	3.0(3)
Li(3)	0.817(5)	-0.120(6)	0.622(3)	0.8(2)
O(1)	0.158(1)	-0.125(1)	0.358(1)	0.28(3) <sup>a</sup>
O(2)	0.438(1)	-0.128(1)	0.887(1)	0.28(3)
O(3)	0.693(1)	-0.118(1)	0.371(1)	0.28(3)
O(4)	0.941(1)	-0.106(1)	0.886(1)	0.28(3)

$$R_N = 100[\Sigma|I(\text{obs}) - I(\text{cal})|/\Sigma I(\text{obs})] = 8.3$$

$$R_p = 100[\Sigma|y(\text{obs}) - y(\text{cal})|/\Sigma y(\text{obs})] = 9.7$$

$$R_w = 100[\Sigma w\{y(\text{obs}) - y(\text{cal})\}^2/\Sigma wy^2(\text{obs})]^{1/2} = 12.3$$

$$R_E = 100[(N - P + C)/\Sigma wy^2(\text{obs})]^{1/2} = 7.5$$

In the above formulas,  $N$  is the number of statistically independent observations,  $P$  the number of parameters refined,  $C$  the number of constraints,  $I$  the integrated intensities,  $y(\text{obs})$  and  $y(\text{cal})$  the observed and calculated intensities, and  $w$  the weights associated with the data points  $y(\text{obs})$ .

*Note.* Numbers in parentheses are standard deviations in the last decimal figure. Space group:  $C2/c$ ,  $Z = 8$ , calculated density  $d_1 = 5.87 \text{ g cm}^{-3}$ . Lattice parameters:  $a_1 = 8.500(3)$ ,  $b_1 = 8.500(3)$ ,  $c_1 = 9.344(3) \text{ \AA}$ ,  $\beta_1 = 117.05(2)^\circ$ .

<sup>a</sup> The oxygen atoms were constrained to have a common temperature factor.

observed profiles together with the plots of the corresponding residuals.

### (b) $\alpha$ -Phase

The Laue symmetry of the  $\alpha$ -phase of  $\text{Li}_3\text{TaO}_4$ , determined by single-crystal X-ray diffraction, is  $2/m$ . A statistical analysis of the measured intensities, performed by computing the average values of several functions of the normalized structure factor  $E$  and by comparing them with the corresponding expected values (9), showed clearly that the crystal is acentric (Table III). No systematic absences were observed, and therefore, the possible space groups for the structure are  $P2$  and  $Pm$ . A

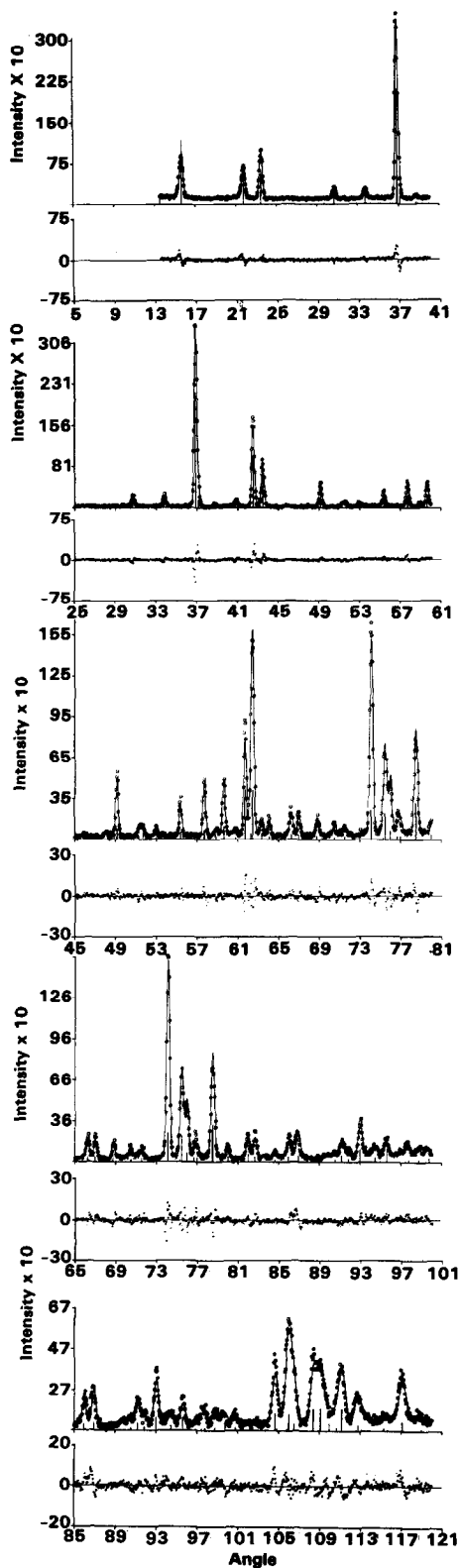


TABLE III  
AVERAGE VALUES OF VARIOUS FUNCTIONS OF THE  
NORMALIZED STRUCTURE FACTOR  $E$  AND  
CORRESPONDING EXPECTED VALUES

Function	Average value	Expected value	
		Acentric	Centric
$ E $	0.882	0.886	0.798
$E^2$	1.000	1.000	1.000
$ E^3 $	1.338	1.329	1.596
$E^4$	2.043	2.000	3.000
$ E^5 $	3.484	3.323	6.383
$E^6$	6.539	6.000	15.000
$ E^2 - 1 $	0.737	0.736	0.968
$(E^2 - 1)^2$	1.043	1.000	2.000
$(E^2 - 1)^3$	2.411	2.000	8.000
$( E^2 - 1 )^3$	2.831	2.415	8.691

three-dimensional Patterson map, calculated using all reflections, showed no important peaks of type  $0y0$  and one outstanding peak of type  $x0z$ . These observations show that the space group can be unequivocally identified as  $P2$ .

The lattice parameters necessary for the intensity measurements were determined with the X-ray four-circle diffractometer using 25 high-angle reflections. These parameters, shown in Table IV, are related to those of the  $\beta$ -phase, and the transformation matrix from the lattice  $H$  of the  $\alpha$ -phase to the lattice  $L$  of the  $\beta$ -phase is

$$S_{hl} = (\bar{1} \bar{1} 0/1 \bar{1} 0/\frac{1}{2} \frac{1}{2}).$$

The lattice  $H$  of the  $\alpha$ -phase is consistent with a pseudo-tetragonal superlattice  $T'$  which can be obtained from  $H$  with the transformation

$$S_{ht'} = (1 0 0/0 1 0/1 0 2).$$

The lattice  $T'$  is the pseudo-tetragonal lattice referred to by Martel and Roth (4) in

FIG. 1. Observed and calculated profiles of the neutron powder diffraction pattern of  $\beta$ - $\text{Li}_3\text{TaO}_4$ , with the corresponding residuals.

TABLE IV  
RESULTS OF THE RIETVELD REFINEMENT OF THE  
STRUCTURE OF  $\alpha$ -Li<sub>3</sub>TaO<sub>4</sub>

Atom	Position	x	y	z
Ta(1)	1(c)	0.5	0	0
Ta(2)	2(e)	0.867(6)	0.186(8)	0.169(3)
Ta(3)	2(e)	0.636(5)	0.450(7)	0.332(3)
Ta(4)	1(b)	0	0.736(10)	0.5
Li(11)	1(a)	0	0.532(20)	0
Li(12)	2(e)	0.340(12)	0.747(12)	0.165(8)
Li(13)	2(e)	0.209(11)	-0.023(11)	0.349(7)
Li(14)	1(d)	0.5	0.233(20)	0.5
Li(21)	1(a)	0	-0.008(30)	0
Li(22)	2(e)	0.332(10)	0.220(12)	0.141(3)
Li(23)	2(e)	0.163(11)	0.476(12)	0.336(8)
Li(24)	1(d)	0.5	0.741(25)	0.5
Li(31)	1(c)	0.5	0.448(22)	0
Li(32)	2(e)	0.847(10)	0.720(11)	0.163(7)
Li(33)	2(e)	0.629(11)	-0.047(10)	0.332(7)
Li(34)	1(b)	0	0.182(19)	0.5
O(1)	2(e)	0.262(6)	0.206(8)	-0.013(3)
O(2)	2(e)	0.268(8)	0.726(11)	0.006(3)
O(3)	2(e)	0.075(8)	-0.018(8)	0.170(4)
O(4)	2(e)	0.590(9)	-0.019(8)	0.157(3)
O(5)	2(e)	0.066(5)	0.452(10)	0.158(3)
O(6)	2(e)	0.598(8)	0.446(9)	0.179(3)
O(7)	2(e)	0.439(6)	0.216(8)	0.335(3)
O(8)	2(e)	0.902(6)	0.219(11)	0.327(3)
O(9)	2(e)	0.426(7)	0.690(9)	0.328(4)
O(10)	2(e)	0.902(7)	0.693(9)	0.340(3)
O(11)	2(e)	0.235(8)	-0.038(11)	0.493(4)
O(12)	2(e)	0.235(8)	0.489(8)	0.507(3)

$R_N = 7.0$ ,  $R_P = 7.2$ ,  $R_W = 9.5$ ,  $R_E = 5.0^a$

Note. Numbers in parentheses are standard deviations in the last decimal figure. Space group:  $P2_1$ ,  $Z = 6$ , calculated density  $d_h = 5.87 \text{ cm}^{-3}$ . Lattice parameters: (i) X-ray measurements,  $a_h = 6.027(2)$ ,  $b_h = 6.004(2)$ ,  $c_h = 12.822(4) \text{ \AA}$ ,  $\beta_h = 103.60(2)^\circ$ . (ii) Neutron refinement,  $a_h = 6.018(1)$ ,  $b_h = 5.995(1)$ ,  $c_h = 12.865(2) \text{ \AA}$ ,  $\beta_h = 103.53(1)^\circ$ . The differences between the lattice parameters determined by X-ray and neutron diffraction may be due to calibration errors.

<sup>a</sup> For the definition of the  $R$  factors, see Table II.

their first report on the existence of the  $\alpha$ -phase of Li<sub>3</sub>TaO<sub>4</sub> and does not have to be confused with the pseudo-tetragonal lattice  $T$  used by Blasse (*J*) to describe the struc-

ture of the low-temperature phase  $\beta$ . This can be obtained from  $T'$  by means of the transformation

$$S_{T'} = (1 \ 0 \ 0/0 \ 1 \ 0/0 \ 0 \ \frac{1}{2}).$$

Several attempts were made to postulate structural models of the  $\alpha$ -phase consistent with the symmetry of space group  $P2_1$ , the geometry of the unit cell, and the main features of the Patterson map. In building these models, it is convenient to start with the atomic arrangement of the  $\beta$ -phase, since the lattice parameters of the two modifications clearly indicate that the two structures must be related to one another.

A projection of the  $\beta$ -phase structure along the  $b_i$  axis of the pseudo-tetragonal cell is shown in Fig. 2. In the figure the monoclinic cell of the  $\alpha$ -phase is also outlined. The projection shows that the  $\beta$ -phase has a periodicity along the  $c_h$  axis four times larger than the period  $c_h$ . A structure with the required  $c_h$  parameter can be obtained from the  $\beta$ -phase by disordering, in equal proportions, the distribution of the Ta<sup>5+</sup> and Li(2)<sup>+</sup> ions. Such model is consistent with the symmetry of space group  $P2_1$  and is also reasonable from a chemical point of view, since the Ta<sup>5+</sup> and Li(2)<sup>+</sup> ions have similar environments and anomalously high-temperature factors in the  $\beta$ -phase. A statistical distribution of Ta<sup>5+</sup> and Li(2)<sup>+</sup> ions, however, is inconsistent with the Patterson map, because it would imply the presence of an important peak at  $\frac{1}{2} \frac{1}{2} 0$  which is not observed. Other possible disordered models can be excluded on similar grounds.

Most of the ordered models consistent with the symmetry  $P2_1$  and the periodicity of the axis  $c_h$  give calculated Patterson maps in general agreement with the map derived from the observed X-ray intensities. The only model giving fairly good agreement between the calculated structure factors and those determined by X rays was one characterized by a chain of Ta<sup>5+</sup> ions of confor-

mation  $t g^+ g^+ t g^- g^-$ .<sup>2</sup> This model was refined with the oxygen ions in approximately the same positions found for the  $\beta$ -phase and with the  $\text{Li}^+$  ions at the centers of the unoccupied oxygen octahedra. In the refinement based on X-ray intensities, only the  $\text{Ta}^{5+}$  positional parameters and an overall temperature factor were allowed to vary. The  $R$  factor obtained after three cycles of calculations was 23%. The model was then refined using the neutron powder data, and the  $R$  factors decreased to quite satisfactory values. The results of these calculations are given in Table IV. Figure 3 shows the observed and calculated profiles with the corresponding residuals, and Fig. 4 illustrates schematically the structure projected on the plane (010).

## Description of the Structures

### (a) $\beta$ -Phase

As pointed out by Blasse (1), the  $\beta$ -phase has the NaCl-type structure in which the cations and the anions are octahedrally coordinated. The ordering of the  $\text{Li}^+$  and  $\text{Ta}^{5+}$  ions along the  $c_t$  axis of the pseudo-tetragonal cell forms a sequence . . . Ta–Li(1)–Li(2)–Li(3)–Ta . . . , and each set of crystallographically equivalent cations forms a chain of conformation  $t g^+ t g^-$  (in Fig. 2 one of these chains has been outlined). The axes of the chains formed by the  $\text{Ta}^{5+}$  and  $\text{Li}(2)^+$  ions are parallel to the direction [001] of the monoclinic reference system, while the axes of the chains formed by the remaining  $\text{Li}^+$  ions are parallel to the direction [101]. The cation–cation distances along the chains are similar for  $\text{Li}(1)^+$  and

<sup>2</sup> These chains are outlined in Fig. 4. The symbols  $t$ ,  $g^+$ , and  $g^-$  are defined in the following way (10): given three successive links  $L_1$ ,  $L_2$ , and  $L_3$ , then  $t$ ,  $g^+$ , or  $g^-$  will be attributed to  $L_2$  if the torsion angle about  $L_2$  is 180, +60, or –60°, respectively. The signs + or – apply if  $L_1$  must be rotated 60° clockwise or counterclockwise (looking from  $L_1$  to  $L_2$ )<sup>1</sup> in order to superpose it to  $L_3$ .

$\text{Li}(3)^+$  [2.95(6) and 2.94(4) Å for  $\text{Li}(1)^+$  and 3.12(8) and 2.91(5) Å for  $\text{Li}(3)^+$ ], while they are significantly different for  $\text{Li}(2)^+$  and  $\text{Ta}^{5+}$  [3.35(9) and 2.98(7) for  $\text{Li}(2)^+$  and 3.15(3) and 2.95(2) for  $\text{Ta}^{5+}$ ]. This feature is not surprising if one considers that  $\text{Ta}^{5+}$  and  $\text{Li}(2)^+$  on one side, and  $\text{Li}(1)^+$  and  $\text{Li}(3)^+$  on the other, have similar coordination spheres.<sup>3</sup> On the same basis, it is not surprising that  $\text{Ta}^{5+}$  and  $\text{Li}(2)^+$  [as well as  $\text{Li}(1)^+$  and  $\text{Li}(3)^+$ ] have similar thermal behavior [in particular, as noted before, the thermal parameters of  $\text{Ta}^{5+}$  and  $\text{Li}(2)^+$  are both abnormally high].

Table V gives selected interatomic distances. The oxygen octahedra are distorted, and the values reported in the table show that the dispersion of the O–O distances is an order of magnitude greater than the estimated standard deviations on the distances themselves. It may also be interesting to note that the distances O(1)–O(1') and O(4)–O(4') between oxygen ions constituting common edges of the coordination octahedra of  $\text{Ta}^{5+}$  ions are significantly shorter than the average of all the O–O distances. Since these short distances occur only in the case of the edge-sharing coordination octahedra of  $\text{Ta}^{5+}$  ions, one may infer that this atomic arrangement in the structure has the function of decreasing the electrostatic repulsion between closely located and highly charged  $\text{Ta}^{5+}$  ions. Finally, the data in Table V show that the average size of the  $\text{Ta}^{5+}$  octahedra is smaller than that of the  $\text{Li}^+$  octahedra.

### (b) $\alpha$ -Phase

The structure of the  $\alpha$ -form can be best described in relation to that of the  $\beta$ -phase. The shifts of the  $\text{Ta}^{5+}$  ions necessary to go from one structure to the other are indicated in Fig. 2, where they are expressed as

<sup>3</sup> The distribution of ions in the second coordination sphere for  $\text{Ta}^{5+}$  and  $\text{Li}(2)^+$  is  $2\text{Ta}^{5+}$ ,  $4\text{Li}(1)^+$ ,  $2\text{Li}(2)^+$ , and  $4\text{Li}(3)^+$ , while for  $\text{Li}(1)^+$  and  $\text{Li}(3)^+$  it is  $4\text{Ta}^{5+}$ ,  $2\text{Li}(1)^+$ ,  $4\text{Li}(2)^+$ , and  $2\text{Li}(3)^+$ .

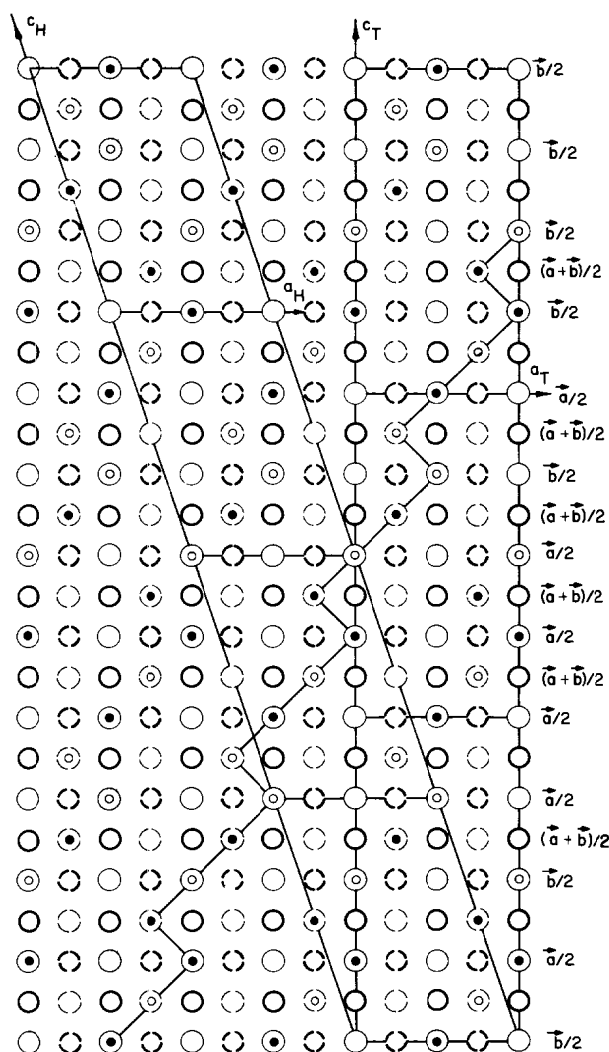
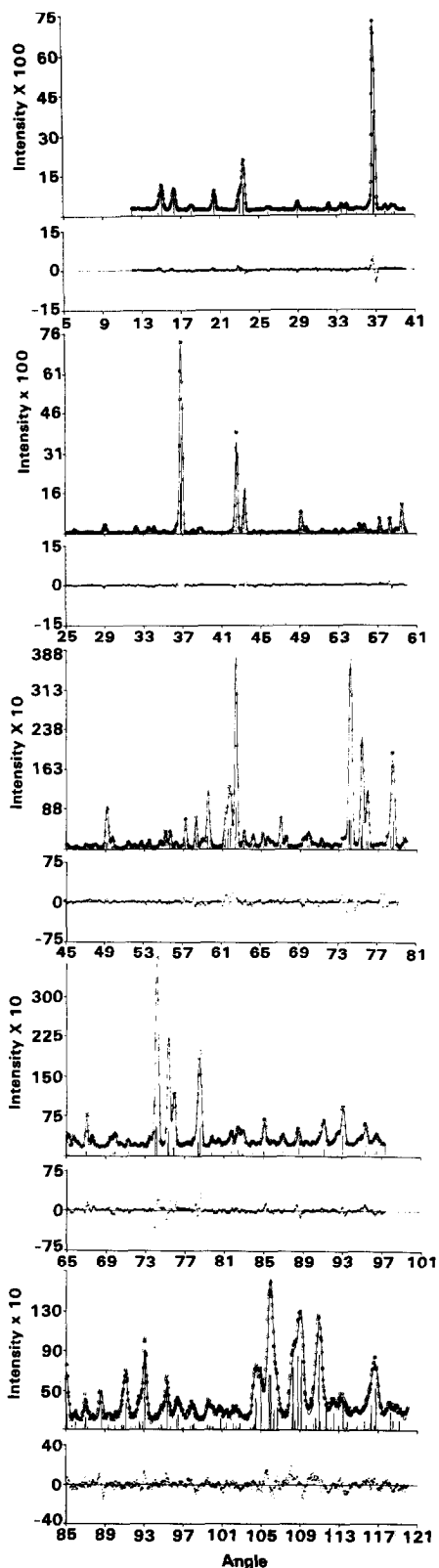


FIG. 2. Idealized structure of  $\beta$ - $\text{Li}_3\text{TaO}_4$  projected along the axis  $b_1$  of the pseudo-tetragonal cell T (see text). The heavy-lined large circles represent oxygen ions at 0 and  $\frac{1}{2}$  (solid line) or  $\frac{1}{4}$  and  $\frac{3}{4}$  (dashed line) along  $b_1$ . The light-lined circles are lithium ions again at 0 and  $\frac{1}{2}$  (solid line) or  $\frac{1}{4}$  and  $\frac{3}{4}$  (dashed line). The small circles represent the tantalum ions. If  $y_1(\text{Ta}) > y_1(\text{Li})$ , the circle representing  $\text{Ta}^{5+}$  is shaded. Four cells of the  $\alpha$ -phase and three pseudo-tetragonal cells T are also outlined. The zigzag line represents the projection of one of the  $t g^+ t g^-$  chains of  $\text{Ta}^{5+}$ . The shifts of the  $\text{Ta}^{5+}$  ions necessary to generate the structure of the  $\alpha$ -phase from the  $\beta$ -phase are indicated at the right side of the figure.

fractions of the parameters  $a_1$  and  $b_1$  of the pseudo-tetragonal cell. All the shifts occur within layers perpendicular to the  $c_1$  axis, and their sequence has a repeat period  $d = 3c_1$ . In this sense,  $d$  may be considered as a parameter representing the pattern of the

transformation in the direction parallel to  $c_1$ . Such pattern does not have any inversions, and this is the reason why the space group changes from  $C2/c$  to  $P2$  in going from the  $\beta$ - to the  $\alpha$ -phase. As can be seen from Fig. 2, odd layers (i.e., the layers at



$c_t/8, 3c_t/8, \dots$ ) either remain unchanged or shift by  $(a_t + b_t)/2$ . Even layers, on the other hand, may remain unchanged or shift by  $a_t/2$  or  $b_t/2$ . The resulting arrangement of the  $Ta^{5+}$  ions gives the chains  $t g^+ g^+ t g^- g^-$  mentioned previously (it is worthwhile to mention that the  $Li^+$  ions also could be connected in a similar way). The axes of the chains are parallel to the direction  $[101]$  of the monoclinic cell of axes  $a_h, b_h,$  and  $c_h$ .

Selected interatomic distances are given in Table VI. In the  $\alpha$ -modification there are no significant differences among the Ta-Ta interatomic distances along the chains (differences in the Li-Li interatomic distances cannot be discussed meaningfully because of the large standard deviations). This finding is in contrast to the case of the  $\beta$ -phase discussed above. The sequences of cations along the direction  $c_t$  of the pseudo-tetragonal cell are of type  $\dots Ta-Li-Li-Li-Li-Li-Ta \dots$  for Ta(1) and Ta(4), and  $\dots Ta-Li-Ta-Li-Li-Li-Ta \dots$  for Ta(2) and Ta(3).

As in the previous case, in the  $\alpha$ -phase the distances between the oxygen ions forming the common edges of the coordination octahedra of the  $Ta^{5+}$  ions are shorter than the average of all the O-O distances.

The average values of the  $M-O$  distances ( $M = Li^+$  or  $Ta^{5+}$ ) reported in Table VII show that the average size of the  $Ta^{5+}$  octahedra is smaller than the corresponding size of the  $Li^+$  octahedra. A similar result has been found for the  $\beta$ -phase, as noted previously. Finally, the data in the table show that also in the case of  $\alpha-Li_3TaO_4$  the oxygen octahedra are, in most cases, significantly distorted.

## Discussion

The transformation from the  $\beta$ - to the  $\alpha$ -phase is sluggish and occurs without

FIG. 3. Observed and calculated profiles of the neutron powder diffraction pattern of  $\alpha-Li_3TaO_4$  and the corresponding residuals.



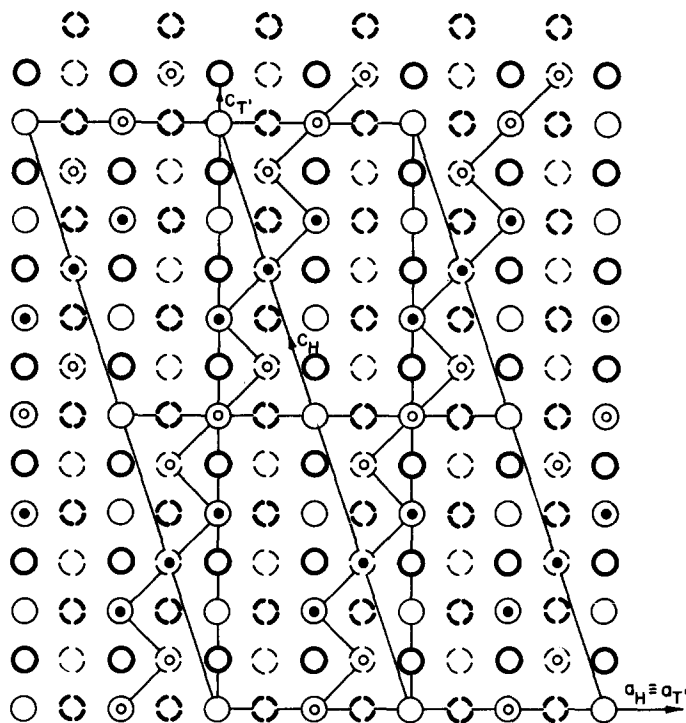


FIG. 4. Idealized structure of  $\alpha$ - $\text{Li}_3\text{TaO}_4$  projected along the axis  $b_1$ , of the pseudo-tetragonal cell  $T'$  (see text). The cell  $T'$  is outlined together with four monoclinic cells  $H$ . The zigzag lines represent the projections of the chains of  $\text{Ta}^{5+}$  ions which have a configuration  $t g^+ g^+ t g^- g^-$ . All symbols are identical to those defined for Fig. 2.

TABLE V  
SELECTED INTERATOMIC DISTANCES ( $\text{\AA}$ ) IN  $\beta$ - $\text{Li}_3\text{TaO}_4$

		$M$	$\overline{M-O}^b$	$\Delta^c$	$\sigma(\Delta)$	Coordination sphere
Ta-Ta' <sup>a</sup>	3.15(3)	Ta	2.004	0.128	0.025	1st
Ta-Ta''	2.95(2)	Li(1)	2.162	0.374	0.045	1st
Li(1)-Li(1')	2.96(4)	Li(2)	2.176	0.548	0.048	1st
Li(1)-Li(1'')	2.95(6)	Li(3)	2.138	0.323	0.066	1st
Li(2)-Li(2')	3.35(9)	O(1)	2.965	0.711	0.025	2nd
Li(2)-Li(2'')	2.98(7)	O(2)	3.015	0.247	0.021	2nd
Li(3)-Li(3')	2.91(5)	O(3)	3.016	0.450	0.022	2nd
Li(3)-Li(3'')	3.12(8)	O(4)	2.966	0.648	0.031	2nd
O(1)-O(1')	2.54(2)					
O(4)-O(4'')	2.60(2)					

Note. Numbers in parentheses are standard deviations in the last decimal figure.

<sup>a</sup> Primed symbols refer to sites transformed by the operation of the twofold axis, and double primed symbols refer to sites transformed by the inversion operation.

<sup>b</sup> These are averages of distances between the ion  $M$  and the 6 (for first coordination sphere) or 12 (for second coordination sphere) anions constituting the coordination sphere.

<sup>c</sup> Dispersion of the  $M$ -O distances and  $\sigma(\Delta)$  is the standard deviation on  $\Delta$ . The ratio  $\Delta/\sigma(\Delta)$  is taken as a measure of the distortion of the corresponding coordination sphere.

TABLE VI  
SELECTED INTERATOMIC DISTANCES ( $\text{\AA}$ ) IN  
 $\alpha\text{-Li}_3\text{TaO}_4$

	$M$	$\overline{M-Li}$	$\Delta^a$	$\sigma(\Delta)^a$	
Ta(1)-Ta(2)	3.10(4)	Ta(1)	2.907	0.303	0.079
Ta(2)-Ta(3)	3.19(3)	Ta(2)	3.031	0.493	0.099
Ta(3)-Ta(4)	3.19(4)	Ta(3)	3.025	0.385	0.099
O(1)-O(4)	2.61(6)	Ta(4)	2.984	0.646	0.113
O(6)-O(8)	2.69(3)				
O(10)-O(12)	2.61(5)				

<sup>a</sup> Defined in Table V.

Note. The average O-O distance, taken on all the O-O distances, is 2.991  $\text{\AA}$ . Numbers in parentheses are standard deviations in the last decimal figure.

change of volume. (The densities calculated for the two phases and reported in Tables II and IV are, in fact, equal.) Tables V and VII also show that the average size of the  $\text{Ta}^{5+}$  and  $\text{Li}^+$  coordination octahedra does not change during the transformation.

As mentioned previously, Fig. 2 shows

TABLE VII  
AVERAGE SIZES OF THE OXYGEN COORDINATION  
OCTAHEDRA IN  $\alpha\text{-Li}_3\text{TaO}_4$

$M$	$\overline{M-O}$	$\Delta$	$\sigma(\Delta)$
Ta(1)	1.986	0.253	0.071
Ta(2)	2.011	0.529	0.064
Ta(3)	2.002	0.300	0.064
Ta(4)	2.010	0.057	0.071
Li(11)	2.185	0.567	0.103
Li(12)	2.173	0.413	0.139
Li(13)	2.188	0.672	0.123
Li(14)	2.187	0.194	0.064
Li(21)	2.152	0.183	0.126
Li(22)	2.147	0.493	0.074
Li(23)	2.156	0.230	0.060
Li(24)	2.149	0.153	0.075
Li(31)	2.148	0.219	0.057
Li(32)	2.161	0.189	0.074
Li(33)	2.153	0.347	0.069
Li(34)	2.147	0.361	0.136

Note. Distances are given in  $\text{\AA}$ ngstroms. The definitions of  $\Delta$  and  $\sigma(\Delta)$  have been given in Table V.

schematically how the  $\text{Ta}^{5+}$  ions have to be shifted in order to produce the structure of the  $\alpha$ -phase from that of the  $\beta$ -phase. These shifts have been introduced formally to describe the relationship between the two modifications of  $\text{Li}_3\text{TaO}_4$ . They might well be, however, the real paths followed by the  $\text{Ta}^{5+}$  ions during the transformation. If this is so, no two consecutive layers or rows of ions would move in the same direction and this complex pattern of shifts would constitute a sort of cooperative motion of ions leading to the  $\alpha$ -modification from the  $\beta$ -form.

It is well known that the presence in a structure of anionic octahedra sharing edges introduces unfavorable electrostatic repulsion between the central metal ions and that the resulting stress depends on the charge on the cations. The stress can be relieved by increasing the distance between the cations. In the structure of  $\beta\text{-Li}_3\text{TaO}_4$ , one of the two Ta-Ta distances along the  $t g^+ t g^-$  chains has a value of 2.95(2)  $\text{\AA}$ , i.e., is significantly less than the other Ta-Ta distance along the same chain (3.15  $\text{\AA}$ ). On the contrary, in the  $\alpha$ -phase the  $\text{Ta}^{5+}$  ions are arranged so that no Ta-Ta distance is shorter than 3.10  $\text{\AA}$ , and their average distance is 3.16  $\text{\AA}$ . The stress introduced by the edge-sharing octahedra, therefore, is smaller in the  $\alpha$ -phase than in the  $\beta$ . This reduction of stress may well be one of the driving forces leading to the transformation observed in the title compound.

## References

1. G. BLASSE, *Z. Anorg. Allg. Chem.* Band **331**, 44 (1964).
2. A. V. LAPICKY AND JU. P. SIMANOV, cited in *Struct. Rep.* **17**, 392 (1953).
3. P. P. PFEIFFER, thesis, Technische Hochschule, Karlsruhe (1963), cited in Ref. (1).
4. L. C. MARTEL AND R. S. ROTH, *Bull. Amer. Ceram. Soc.* **60**, 376 (1981).
5. E. PRINCE AND A. SANTORO, in "National Bureau

- of Standards, U.S. Technical Note 1117" (F. Shorten, Ed.) (1980).
6. H. M. RIETVELD, *J. Appl. Crystallogr.* **2**, 65 (1969).
  7. E. PRINCE, in "National Bureau of Standards U.S. Technical Note 1117" (F. Shorten, Ed.) (1980).
  8. G. E. BACON, *Acta Crystallogr. Sect. A* **28**, 357 (1972).
  9. I. L. KARLE, K. BRITTS, AND P. GUM, *Acta Crystallogr.* **17**, 496 (1964).
  10. P. CORRADINI, in "The Stereochemistry of Macromolecules" (A. D. Ketley, Ed.), Vol. 3, Dekker, New York (1968).